Comparisons of sets of electron–neutral scattering cross sections and swarm parameters in noble gases: I. Argon

2013 J. Phys. D: Appl. Phys. 46 334001

(http://iopscience.iop.org/0022-3727/46/33/334001)

J. Phys. D: Appl. Phys. **46** (2013) 334001 (19pp) doi:10.1088/0022-3727/46/33/334001

Comparisons of sets of electron–neutral scattering cross sections and swarm parameters in noble gases: I. Argon

L C Pitchford[1,2], L L Alves[3], K Bartschat[4], S F Biagi[5], M C Bordage[1,2], A V Phelps[6,10], C M Ferreira[3], G J M Hagelaar[1,2], W L Morgan[7], S Pancheshnyi[1,2], V Puech[8], A Stauffer[9] and O Zatsarinny[4]

[1] Université de Toulouse; UPS, INPT; LAPLACE (Laboratoire Plasma et Conversion d'Energie); 118 route de Narbonne, F-31062 Toulouse cedex 9, France
[2] CNRS; LAPLACE; F-31062 Toulouse, France
[3] Instituto de Plasmas e Fusão Nuclear, Instituto Superior Técnico, Universidade Técnica de Lisboa, Av. Rovisco Pais, 1049-001 Lisboa, Portugal
[4] Department of Physics and Astronomy, Drake University, Des Moines, IA 50311, USA
[5] University of Liverpool, Oliver Lodge Laboratory, Oxford St., Liverpool L69 7ZE, UK
[6] JILA, NIST and University of Colorado, Boulder, CO 80309–0440, USA
[7] Kinema Research and Software, PO Box 1146, Monument, CO 80132, USA
[8] Laboratoire de Physique des Gaz et des Plasmas, CNRS & Univ. Paris-Sud F-91405, Orsay, France
[9] Department of Physics and Astronomy, York University, Toronto, ON M3J 1P3, Canada

E-mail: pitchford@laplace.univ-tlse.fr

Received 24 April 2013, in final form 30 June 2013
Published 5 August 2013
Online at stacks.iop.org/JPhysD/46/334001

Abstract
This paper describes work done in the context of the Gaseous Electronics Conference (GEC) Plasma Data Exchange Project (PDEP) as discussed in the preface to this cluster issue. The purposes of this paper and its companion papers are to compare sets of cross sections for electron scattering from ground-state noble gas atoms in the energy range from thermal to about 1 keV and to comment on their applicability for plasma modelling. To these ends, we present in this paper intercomparisons of the nine independently derived sets of cross sections for electron scattering from ground-state argon atoms that have been posted in databases on the LXCat open-access website (www.lxcat.laplace.univ-tlse.fr). We show electron transport, excitation and ionization coefficients (swarm parameters) calculated using these cross section data in Boltzmann solvers and we compare calculated values with measurements. For the most part, the cross section sets have been compiled by co-authors on this paper and appendices giving details about how the various cross sections datasets were compiled have been written by the individual co-authors. Additional appendices discuss our criteria for selection of experimental data to be included in the comparisons and give a brief overview of the methods used here for solving the Boltzmann equation.

(Some figures may appear in colour only in the online journal)

1. Introduction

According to the 2012 Plasma Roadmap, '[Numerical] modelling of low-temperature plasmas is increasingly viewed as a scientific tool on a par with experiments' (Samukawa *et al* 2012), although it is perhaps harder for the modeller to argue convincingly that the results obtained respond correctly to the problem being posed. This is all the more difficult for users of commercial codes. The integrity of the results obtained from numerical modelling depends on the identification of a physical model appropriate for addressing the problem of interest, on a good choice and proper implementation of the numerical solution techniques, and on the availability of reliable input

[10] Deceased.

data. The Gaseous Electronics Conference established the Plasma Data Exchange Project (PDEP) to address the latter issue—availability of reliable data—as discussed in the preface to this cluster issue.

In the context of the PDEP, this paper and its companion papers in this cluster issue are focused on data related to the electron component in low-temperature plasmas in noble gases. Such data are fundamental because the electrons are the primary means through which energy from the electromagnetic fields sustaining the plasma is coupled to the neutral gas. Input data needed for plasma modelling depend on the questions being addressed and how the model has been formulated, but in general the requirement is for a complete set of electron–neutral scattering cross sections. We use 'complete' here to mean that the cross section set represents well all electron energy and momentum losses as well as the electron number changing processes or ionization and attachment (Petrović *et al* 2009). Obviously, in different contexts, there could be other criteria for defining a 'complete' set of cross sections (Gargioni and Grosswendt 2008).

A large body of data is available in the literature reporting measurements or calculations of electron–argon scattering cross sections, both total and differential scattering cross sections, but the publications often focus on one or a subset of the important scattering processes. For a recent, comprehensive review in argon see (Gargioni and Grosswendt 2008). A task of the plasma modeller is to assemble the requisite input data from this large body of sometimes disparate, contradictory or incomplete information in the literature.

A common approach for evaluating the completeness of a cross section set is to use it as input in a calculation of the steady-state, equilibrium distribution function of electrons subjected to the combined influences of a uniform electric field and collisions with a uniform number density of neutral, ground-state target species. Integrals over the electron energy distribution function (eedf) yield macroscopic quantities such as drift velocity, diffusion coefficients and ionization coefficients (e.g. 'swarm' parameters) which can be measured with high precision. Swarm parameters are measured at very low currents to assure that the electrons interact only with neutral gas atoms/molecules in their ground state at controlled temperature, and much experimental effort has been devoted to creating conditions where local equilibrium exists between electron momentum and energy loss in collisions and electron acceleration in the field so that the measured swarm parameters are free of boundary effects and independent of space and time. In these conditions, swarm parameters are functions of the reduced electric field strength, E/N, the ratio of the electric field strength to the neutral density, and of the composition of the gas (Huxley and Crompton 1974, Dutton 1975, Gallagher *et al* 1983). Putting aside for the moment issues regarding the numerical solution techniques and how to define swarm parameters for given experimental situations, we demand that in order to be complete, the cross section set, when used in a Boltzmann solver, must yield swarm parameters consistent with measured values. 'Consistent' depends on the context (White *et al* 2003), but for the purposes here, consistent means that calculated and measured swarm parameters agree to well within a few tens of per cent.

In this paper, we discuss nine, independently compiled datasets for electron scattering in argon in the energy range from thermal to some hundreds of eV or 1 keV, depending on the datasets—eight of these are complete in the sense defined above—and, with the exception of the dataset compiled by the late Professor Hayashi, the datasets discussed here were compiled by co-authors on this paper. A couple of these data sets were compiled prior to 1980 but were updated, although irregularly, as new information appeared in the literature. Others were determined very recently, either from theory or by taking into account new measurements. Most have been used in various modelling applications as described in the appendices or in the references. These datasets have all been made available on the open-access website LXCat (www.lxcat.laplace.univ-tlse.fr) where they can be plotted, downloaded, or used in an on-line Boltzmann solver (Pancheshnyi *et al* 2012).

Seven of the nine datasets for electron scattering in argon were compiled through an iterative process involving piecing together a set of cross sections from the literature, evaluating swarm parameters, adjusting if necessary the magnitudes and shapes of the cross sections (within experimental error, if possible) to improve the agreement between calculated and measured swarm data. See Petrović *et al* (2009) for a review of cross section sets that have been determined recently using this approach. These seven complete datasets include cross sections for elastic momentum transfer, total cross sections for excitation of individual or groups of levels (depending on the dataset), and total ionization cross section. Total cross sections correspond to differential cross sections averaged over all scattering angles. Elastic momentum transfer is the $(1-\cos\theta)$ weighted, angle-averaged differential cross section for elastic scattering, where θ is the scattering angle. In the case of N_2, it has been shown that swarm parameters can be calculated to within an acceptable accuracy neglecting higher order anisotropies in the scattering cross sections (Phelps and Pitchford 1985).

The other two of the nine datasets are from quantum calculations—one of these is complete (the BSR dataset in table 1) in the sense described above while the second (the NGFSRDW dataset in table 1) contains data for excitation only but includes cross sections for excitation from the ground state as well as excitation from excited states. Quantum calculations yield fully differential cross sections, but the data on the LXCat site at present are limited to total cross sections for excitation and ionization and momentum-transfer cross sections for elastic scattering. The BSR dataset is of special interest here—in contrast to the seven datasets assembled from multiple sources described in the paragraph above, this theoretical dataset is complete and internally consistent. Similar computational techniques have been used to calculate cross section sets in Ne as discussed in Paper II (Alves *et al* 2013) and in Kr and Xe in as discussed Paper III (Bordage *et al* 2013), although the latter datasets do not include ionization. Detailed quantum calculations, complemented by experimental data, have previously been used in the process

Table 1. Data available on LXCat for electron–argon scattering cross sections. The first column is the database name (chosen by the contributors), the second column is a summary of the contents of the argon dataset, and the third column gives the names of contributors, references and key dates, how the cross sections were determined. More details about the individual datasets are given in the appendices as indicated. Users are requested to cite the LXCat website (www.lxcat.laplace.univ-tlse.fr/) and the references given in the table, in all publications making use of these data. Users are further requested to cite sources of original data (see the appendices) where possible.

Database name	Description of argon dataset	Comments
BIAGI-v7.1	Elastic momentum transfer, ionization, and 3 excitation levels (grouped into S, P and D levels)	Contributor: S F Biagi References: BIAGI-v7.1 database, www.lxcat.laplace.univ-tlse.fr; Transcribed from SF Biagi's Fortran code MAGBOLTZ, Version 7.1, 2004. http://consult.cern.ch/writeup/magboltz. Swarm-derived cross section set developed using a Monte Carlo simulation for calculation of swarm parameters. See appendix A.
BIAGI-v8.9	Elastic momentum transfer, ionization, and 44 excitation levels	Contributor: S F Biagi References: BIAGI-v8.9 database, www.lxcat.laplace.univ-tlse.fr; Transcribed from SF Biagi's Fortran code MAGBOLTZ, Version 8.97, 2011. http://consult.cern.ch/writeup/magboltz. Swarm-derived cross section set developed using a Monte Carlo simulation for calculation of swarm parameters. See appendix A.
BSR	Elastic momentum transfer, ionization, and 30 excitation levels	Contributors: O Zatsarinny and K Bartschat References: BSR database, www.lxcat.laplace.univ-tlse.fr; Calculated using the method described by Zatsarinny and Bartschat (2004) and extended using the same philosophy as for e–Ne described by Zatsarinny and Bartschat (2012a, 2012b). A complete set of theoretical e–Ar cross sections from B-spline R-matrix (BSR) calculations. These cross sections were calculated in 2013 using a close-coupling model with 500 target states, including the lowest 31 physical states and 469 pseudo-states, of which 47 represented the high-lying Rydberg spectrum and 422 the ionization continuum. These data were uploaded to LXCat in February 2013 and replaced a previous set (based on Zatsarinny and Bartschat 2004) uploaded to LXCat in 2011. See appendix B.
HAYASHI	Elastic momentum transfer, ionization, and 25 excitation levels	Reference: HAYASHI database, www.lxcat.laplace.univ-tlse.fr; Hayashi (2003), table 2. Swarm-derived cross section set developed using a Monte Carlo simulation for calculation of swarm parameters. The dataset was developed in 1991. See appendix C. Note that an informally circulated set of cross sections with the same reference represents incorrectly the elastic momentum-transfer cross section.
IST-LISBON	Elastic momentum transfer, ionization, and 37 excitation levels	Contributors: L L Alves and C M Ferreira Reference: IST-LISBON database, www.lxcat.laplace.univ-tlse.fr; Yanguas-Gil *et al* (2005). Swarm-derived cross section set developed using a two-term Boltzmann solver for calculating swarm parameters. Use of these cross sections is appropriate for low E/N (less than some 200 Td) where the influence of the secondary electrons born in ionization events can be neglected. See appendix D.
MORGAN	Elastic momentum transfer, ionization, and 2 excitation levels	Contributor: W L Morgan Reference: MORGAN database, www.lxcat.laplace.univ-tlse.fr. This dataset was developed in the 1970s and was based on the best data available at that time. Swarm-derived cross section set developed using the two-term Boltzmann solver, ELENDIF (Morgan and Penetrante 1990), for calculation of swarm parameters. See appendix E.
NGFSRDW	Partial set of cross sections for excitation of ground and excited states	Contributor: A Stauffer References: NGFSRDW database, www.lxcat.laplace.univ-tlse.fr. Calculated using the method described by Zuo *et al* (1991). A set of excitation cross sections to individual fine-structure levels calculated using a relativistic distorted-wave method which is expected to be accurate for high electron energies but not in the threshold region. To find these in the LXCat database, look for state-specific species names. See appendix F.
PHELPS	Effective momentum transfer, ionization, and 1 effective excitation level	Contributor: A V Phelps Reference: PHELPS database, www.lxcat.laplace.univ-tlse.fr; Based on Frost and Phelps (1964) as modified by Tachibana and Phelps (1981). This dataset was last updated in 1997 and was originally posted by Phelps in his ftp file (Phelps 1997). These data were uploaded to LXCat in 2009. Swarm-derived cross section set developed using the two-term Boltzmann solver, BACKPRO (Luft 1975), for the calculation of swarm parameters. See appendix G.
PUECH	Elastic momentum transfer, ionization, and 40 excitation levels	Contributor: V Puech Reference: PUECH database, www.lxcat.laplace.univ-tlse.fr; Puech and Torchin (1986). Swarm-derived cross section set developed using a two-term Boltzmann solver for calculation of swarm parameters. See appendix H.

of compiling a complete cross section set (see, for example, Ralchenko *et al* (2008) for He and Morgan *et al* (2001) for CHF_3), but never before, to our knowledge, have quantum calculations alone provided a complete dataset.

We will show below that the complete cross section sets presented in this paper are appropriate for use in Boltzmann solvers and calculations of swarm parameters, but that they differ among themselves both in the level of detail taken into account in excitation cross sections and for the cross sections for excitation of specific levels in the cases where it is possible to compare. These data are also expected to be appropriate for use in more complicated situations where there is no local equilibrium between acceleration of electrons in the field and energy and momentum loss in collisions, but this is an issue that merits further study.

The work presented in this cluster issue was originally reported at the 2011 Gaseous Electronics Conference. The present paper discusses cross sections for electron scattering in argon. Cross sections for electron scattering in helium and neon are discussed in Paper II (Alves *et al* 2013) and in krypton and xenon in Paper III (Bordage *et al* 2013). Paper IV (Bartschat 2013) in this series is an overview of theoretical methods for calculations of cross sections for electron–atom scattering. Again, all data discussed in papers I, II and III are available on the LXCat open-access website at www.lxcat.laplace.univ-tlse.fr. Data for electron scattering in other gases are also available on the LXCat website and efforts are continuing towards the evaluation of electron scattering data in other gases. These will be reported separately.

This paper is organized as follows: in section 2, we show intercomparisons of the cross section sets presently available on LXCat. Swarm parameters calculated using these datasets in the two-term Boltzmann equation solver BOLSIG+ (Hagelaar and Pitchford 2005) or in the Monte Carlo simulation package MAGBOLTZ (Biagi 2011) are compared to measurements in section 3. Only a few of the datasets listed in table 1 are well-documented in the literature. Appendices A through H to this article provide more information about how these datasets were derived and tested or about how they should be used. The two additional appendices discuss our choice of experimental data for comparison (appendix I) and the numerical methods used in the calculations presented here (appendix J).

2. Comparisons of cross sections in argon presently available in the LXCat databases

The LXCat website is structured into databases maintained by individual contributors. Table 1 lists all the databases on LXCat containing cross section sets for argon at the time of writing. In the following, we will refer to these datasets by the names in the first column. Note that most of the databases contain datasets not only for argon but for other target species as well. See www.lxcat.laplace.univ-tlse.fr for a description of data for other target species in each database.

Except for the NGFSRDW database, the cross section sets on LXCat for argon are complete and can be used directly in Boltzmann calculations to determine the eedf. These complete

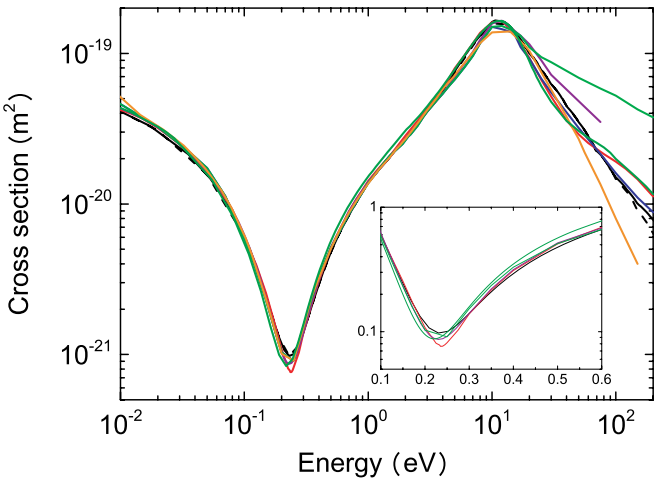

Figure 1. Comparisons of elastic momentum transfer (or effective momentum transfer from PHELPS) cross section versus electron energy in argon from the different databases. The inset is a zoom in the region of the Ramsauer minimum with cross sections in units of 10^{-20} m^2. The colour code is the same for all figures in this article: BIAGI-v8.9 (——); BIAGI-v7.1 (- - - -); BSR (——); HAYASHI (——); IST-LISBON (——); MORGAN (——); PHELPS (——); PUECH (——).

sets include either elastic *momentum transfer*, $Q_{\mathrm{m,el}}$, or, in the case of the PHELPS database, an effective momentum transfer, $Q_{\mathrm{m,eff}}$ (sum of $Q_{\mathrm{m,el}}$ and total cross sections for excitation and ionization). Also included in each are *total* (angle integrated) cross sections for electron impact ionization and excitation from the ground state to excited states. These datasets differ in how the excited states are described—individually or as groups of levels. The NGFSRDW dataset includes *total* cross sections for excitation from the ground state to 40 excited levels as well as *total* cross sections for excitation of the individual 1s and 2p levels to higher 1s and 2p excited states. Recall that the quantum calculations (BSR and NGFSRDW databases) yield differential cross sections for each process, but it is the corresponding total excitation, total ionization and elastic momentum-transfer cross sections that are tabulated on LXCat. The cross sections for total elastic scattering, $Q_{\mathrm{T,el}}$, are presently not included in the datasets on LXCat because this quantity is not used in Boltzmann solvers.

Figure 1 shows the elastic momentum-transfer cross sections, $Q_{\mathrm{m,el}}$, (or $Q_{\mathrm{m,eff}}$ in the case of PHELPS) from the seven swarm-derived cross section datasets and from the quantum calculations of Zatsarinny and Bartschat in the BSR dataset. A zoom of the region near the Ramsauer minimum is shown in the inset in figure 1 where we see that the cross sections agree to within about 10% on the position of the minimum but differ as much as 20% on its depth. The data from PUECH and from IST-LISBON are the same as those from PHELPS in this energy range and the BIAGI-v7.1 data are the same as in BIAGI-v8.9 for $Q_{\mathrm{m,el}}$ in the region of the minimum. Between the Ramsauer minimum and the peak at about 11 eV, there is general agreement among the various datasets. The differences between the highest (BSR) and lowest (BIAGI-v8.9) values of $Q_{\mathrm{m,el}}$ for energies just past the Ramsauer minimum are about 20% and in the 7 eV region, the differences are again about 20% between the highest (BSR) and the lowest

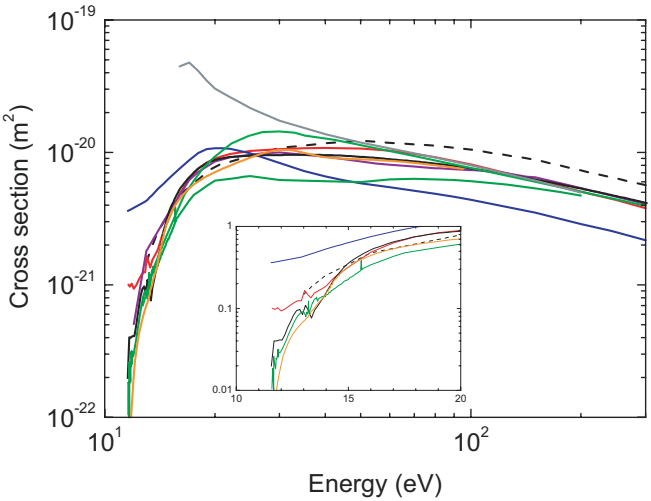

Figure 2. Total excitation cross sections versus energy in argon from the different databases. The inset is a zoom between 10 and 20 eV to show the near-threshold resonance structures, and the unit for the cross sections in the zoom is 10^{-20} m^2. The colour code is: BIAGI-v8.9 (——); BIAGI-v7.1 (- - - -); BSR (——); HAYASHI (——); IST-LISBON (——); MORGAN (——); NGFSRDW (——); PHELPS (——); PUECH (——).

(PHELPS). The more recent compilations are generally a bit higher than the data from PHELPS in this region. The increasing differences between cross sections datasets past the onset of the inelastic channels is not significant for our purposes since the calculated swarm parameters are not very sensitive to $Q_{\mathrm{m,el}}$ at energies past the inelastic thresholds. Recall that the PHELPS data correspond to an effective momentum-transfer cross section and so are not directly comparable to the others after the onset of the inelastic processes at 11.55 eV.

The level of detail included for the inelastic processes in the different databases varies considerably, ranging from one single effective excitation level in the PHELPS database to a detailed description with 44 levels in the recent compilation in the BIAGI-v8.9 database. The total inelastic cross section, Q_{exc}, is therefore the only quantity we can use for intercomparisons of inelastic collisions from all nine of the databases. Plots of Q_{exc} from each dataset are shown together in figure 2.

Let us first look at the total excitation cross section calculated from the two sets of quantum calculations—from the relativistic distorted-wave (RDW) approach in the NGFSRDW database based on the computational method of Zuo *et al* (1991) and from the 2013 B-Spline R-Matrix calculations (unpublished) of Zatsarinny and Bartschat with 500 pseudo-states using the method Zatsarinny and Bartschat (2004). The latter are in the BSR database. The NGFSRDW data are consistent with most of the other datasets at high energy but diverge with decreasing energy. As said in appendix F, the RDW method is expected to yield accurate results at energies higher than several times the excitation thresholds. The BSR calculations, on the other hand, are expected to be accurate in the near-threshold region and the low-energy calculated resonance structure is indeed in good agreement with the experiments of Allan *et al* (2006). The BSR and the RDW calculations converge at high energy as expected. The BSR calculations are lower than the other LXCat datasets from 20 to 200 eV and lower than experiments (see figure 21 in Gargioni and Grosswendt (2008) and appendix B for comments on this point).

The excitation cross sections in the datasets PHELPS, MORGAN, and BIAGI-v7.1 contain one, two, or three excitation levels, respectively, and the magnitudes of these cross sections were first estimated by theory and/or experiment and then adjusted to yield good fits to swarm parameters. We will refer to these as the 'simplified' datasets in the following. The single excitation level with a threshold energy of 11.55 eV in the PHELPS dataset was taken from the measured total excitation cross section of Schaper and Scheibner (1969). The cross sections in the MORGAN dataset correspond to two groups of levels—'allowed' and 'forbidden' levels—both with a threshold of 11.55 eV. The forbidden level is characterized by a lower peak and faster drop with increasing energy past the peak. The BIAGI-v7.1 dataset includes effective levels for excitation of s, p and d levels with thresholds of 11.55 eV, 13 eV and 14 eV, respectively. As we will see below, when used as input to a Boltzmann solver, the three simplified datasets all yield results consistent with swarm experiments and are thus useful when a detailed description of the excitation is not required. The higher total excitation cross section above about 100 eV for BIAGI-v7.1 has very little influence on the swarm parameters presented in the following section because very few electrons attain energies greater than 100 eV for the conditions of interest.

The remaining four datasets (BIAGI-v8.9, HAYASHI, IST-LISBON and PUECH) are attempts to assemble complete sets of electron–argon scattering cross sections from beam measurements and/or theory. We will refer to these as the 'detailed' datasets. In all cases, some modifications or extensions of the literature values were needed to obtain consistency with swarm parameters. The PUECH and HAYASHI datasets were assembled in 1986 and 1992, respectively. At the origin of the PUECH dataset was the compilation by Bretagne *et al* (1986) developed for use in modelling plasmas generated by relativistic electron beams, and Puech and Torchin extended this compilation to lower energies (Puech and Torchin 1986). Unfortunately, we do not have the details about how Hayashi's dataset was constructed or how experimental cross sections were adjusted to yield improved values of the swarm parameters. The measurements by Khakoo *et al* (2004), Weber *et al* (2003) and by Allan *et al* (2006) inspired the recent compilations in the IST-LISBON (Yanguas-Gil *et al* 2005) and BIAGI-v8.9 (Biagi 2011) databases. The IST-LISBON dataset is based mainly on measurements. Only one adjustment was made in order to improve the agreement with measured swarm parameters—a scale factor of 0.5 was applied to the measurements of Khakoo *et al* (2004) for the resonance levels. In 2009, Biagi assembled a new dataset for argon to take into account the latest results from Allan *et al* (2006) for the near-threshold shape and amplitude of the cross sections for excitation of the lower levels. As a result, the sum of the cross section for excitation of the 1s levels is increased near threshold and decreased in the

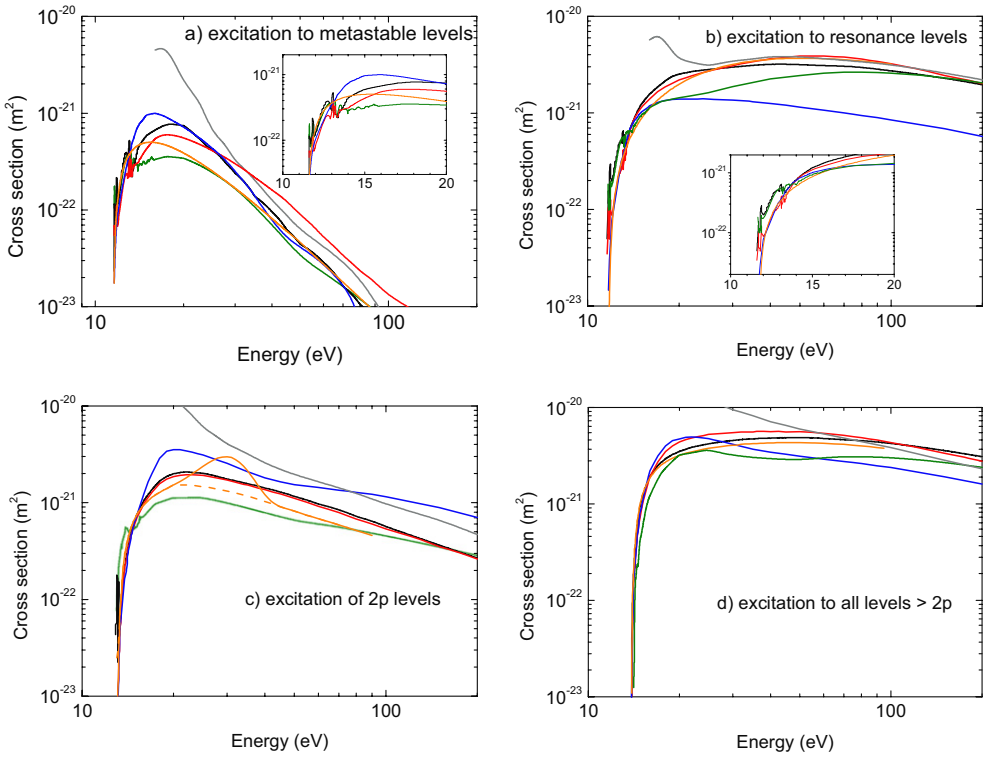

Figure 3. Comparisons of cross sections for (*a*) excitation to metastable levels (*b*) excitation to resonance levels (*c*) excitation to 2p levels; and (*d*) excitation to all higher levels. The colour code is: BIAGI-v8.9 (——); BSR (——); HAYASHI (——); IST-LISBON (——); NGFSRDW (——); PUECH (——). The dashed line in figure 3(*c*) corresponds to the modification of the PUECH dataset as described in the text.

100 eV region as compared to his simplified dataset in BIAGI-v7.1 using one effective level to represent excitation of these four levels.

In figure 3, we compare sums of excitation cross sections from the two sets of quantum calculations and from the four 'detailed' databases for specific groups of levels. The following summed cross sections are shown: figure 3(*a*)—excitation to the metastable levels $1s_5$ (11.55 eV threshold) and $1s_3$ (11.72 eV threshold); figure 3(*b*)—excitation to the resonance levels $1s_4$ (11.62 eV threshold) and $1s_2$ (11.83 eV threshold); figure 3(*c*)—excitation to the ten 2p levels with thresholds between 13.07 and 13.60 eV; figure 3(*d*)—excitation to all levels with thresholds >13.60 eV. All figures are shown on the same scale.

As mentioned above, the RDW calculations in the NGFSRDW database should be valid for energies higher than several times the threshold, but not near threshold. The generally higher level of excitation in the near-threshold region in the calculations of BSR for excitation to metastable and resonance levels—again, consistent with recent experiment—has been incorporated in the BIAGI-v8.9 dataset. In the 20 to 200 eV region, all of the BSR results are lower than in the other databases for curves in figure 3 except for the excitation to the metastable levels. The IST-LISBON data for excitation to the resonance levels in figure 3(*b*) were taken from the experiments of Khakoo *et al* (2004) but rescaled by a factor of 0.5 and are quite a bit lower than the other curves in figure 4(*b*). The IST-LISBON data are higher than the others (except NGFSRDW) for the sum of the 2p cross section in figure 3(*c*). The PUECH curve for excitation of the 2p states has a maximum at about

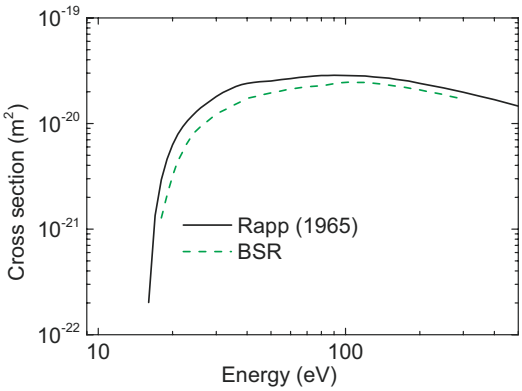

Figure 4. Total ionization cross sections as a function of electron energy. The ionization cross section in the swarm-derived databases are all within a few per cent of the measurements from Rapp and Englander-Golden, shown here compared with the cross section from the quantum calculations in the BSR database.

30 eV which is caused by peaks in the cross sections for excitation to the $2p_{10}$ and $2p_9$ levels. These data were taken from Chutjian and Cartwright (1981) and we question whether or not there is a misprint in the tabulated cross sections for the $2p_{10}$ and $2p_9$ levels at 30 eV. By removing these anomalously high values in the 30 eV region from the PUECH dataset, we arrive at the curve shown in the dashed line in figure 3(*c*) which is sensibly in line with most of the others. The HAYASHI and BIAGI-v8.9 datasets are in reasonable agreement with each other except for the generally higher level of excitation in the near-threshold resonance structure in the BIAGI-v8.9 dataset.

Table 2. List of swarm parameters discussed here with symbols and units.

Parameter	Symbol	Units
Reduced electron mobility	μN (μ is the mobility and N is the neutral gas number density).	$(\mathrm{m\,V\,s})^{-1}$
Ratio of transverse diffusion coefficient to mobility	D_T/μ (D_T is the transverse diffusion). The quantity eD_T/μ (e is the electric charge) is called characteristic energy and is in units of eV.	V
Ratio of longitudinal diffusion coefficient to mobility	D_L/μ (D_L is the longitudinal diffusion coefficient)	V
Reduced ionization coefficient	α_i/N	m^2
Ionization rate coefficient	k_i	$\mathrm{m}^3\,\mathrm{s}^{-1}$
Reduced excitation coefficient	α_exc/N	m^2

The ionization cross sections in the swarm-derived cross section datasets are taken from Rapp and Englander-Golden (1965) except for BIAGI-v8.9 (which is an average of Rapp and Englander-Golden and the more recent measurements of Straub *et al* (1995) and for PUECH who uses measurements of Wetzel *et al* (1987) that are only slightly different from those of Rapp and Englander-Golden. The BSR calculations of Zatsarinny and Bartschat yield an ionization cross section quite a bit lower than that of Rapp and Englander-Golden in the 20 to 100 eV range, as shown in figure 4. This point is discussed in appendix B.

The review paper by Gargioni and Grosswendt (2008) shows comparisons of experimental cross sections in argon over the energy range of interest here. We have not reproduced those comparisons here because our focus is on the data available on LXCat. However, a few comments should be made. Figure 13 in their review paper shows that measurements of $Q_\mathrm{m,el}$ agree within about 30% over the entire energy range. Note that the older swarm-derived data of Frost and Phelps (1964) shown in this figure were later revised (Yamabe *et al* 1983) as included in the PHELPS dataset on LXCat. The curves in figure 13 of the review paper and data in our figure 1 are in good agreement. Figures 18, 14 and 19 in the Gargioni and Grosswendt paper can be compared to our figures 3(*a*), (*b*), and (*c*), respectively, but the spread in the experimental data is too large to allow us to draw conclusions. Experimental determinations of total ionization cross sections are shown in figure 23 of the review paper and can be compared with figure 4 above.

3. Comparisons of electron swarm parameters

The swarm parameters that we will be discussing in this section are summarized in table 2. Recall that these swarm parameters are functions of the local reduced electric field strength, E/N, as discussed in the introduction. The unit used here for E/N is Townsend ($1\,\mathrm{Td} = 10^{-21}\,\mathrm{V\,m}^2$).

Swarm parameters have been measured for many years and some of these data have been transcribed to experimental databases presently available on LXCat as listed in table 3. The experimental data on LXCat for pure noble gases and simple molecular gases are more complete than are the data in complex gases, but further transcription is in progress. We have selected only a few of the available data for comparison here with the calculated values of swarm parameters. The guidelines for selection of experimental data for our comparisons are discussed in appendix I.

Table 3. List of experimental databases available on LXCat.

Database name	Contents
de Urquijo	Data from Hernandez-Avila *et al* (2004)
Dutton	Transcription from Dutton's 1975 review article, 'Survey of Electron Swarm Data'. (Dutton 1975)
IST-Lisbon	Compilations of experimental swarm data, used over the years by the Group of Gas Discharges and Gaseous Electronics with the IPFN/IST, Lisbon, Portugal, to adjust electron–neutral scattering cross section sets in various gases.
LAPLACE	Data published after or not appearing in the 1975 Dutton review. These data were assembled at LAPLACE in Toulouse, France, and are relatively complete for noble and simple atmospheric gases. Additional data are being uploaded regularly. When possible, data were taken from published tables. If the data were digitized from figures, this has been noted in the database.

Note that swarm parameters can be measured in different experimental configurations and not all are equivalent when the electron number density is changing because of ionization (or attachment), for reasons discussed by Tagashira *et al* (1977) and many others. See appendix J. Two simple situations are assumed for the calculations here—'steady-state Townsend' (SST) in which there can be an exponential growth (or decay) of electron current between the electrodes and 'pulsed Townsend' (PT) in which the spatially averaged electron number density can increase (decrease) exponentially in time. The experimental points and all calculations shown here for α_i/N correspond to the SST configuration. We also use SST for the calculations of D_T/μ, μN, and α_exc/N. The results for D_L/μ were calculated for a 'PT' formulation to be more consistent with experiments. This distinction has very little effect on the diffusion coefficients, but μN and α_i/N calculated for SST can differ by about 10% at 500 Td from those calculated by PT. See appendix J for more detail.

In the following, we show only a few results using BIAGI-v7.1 because they are usually within a few per cent of the results calculated using BIAGI-v8.9 between 0.01 and 500 Td.

3.1. Comparison of measured and calculated reduced mobility

Experiments usually measure the electron drift velocity, v_d, which is converted here to a reduced electron mobility through

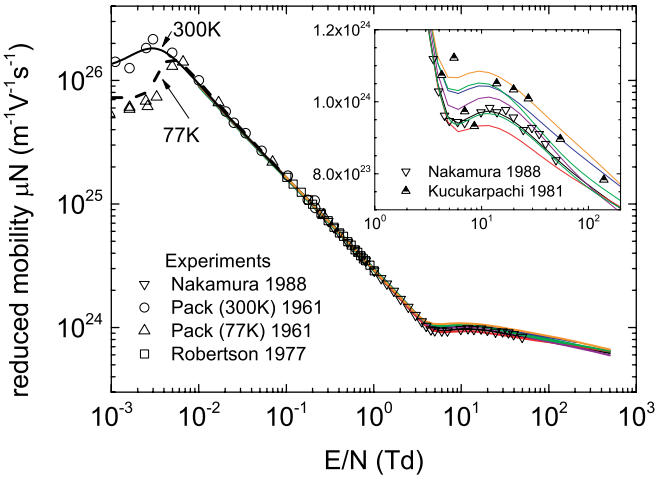

Figure 5. Reduced electron mobility versus E/N. The symbols are experimental data and the solid lines are calculations using the two-term Boltzmann solver, BOLSIG+. The inset is a zoom to illustrate the differences in the calculated results in the region of the knee at $E/N \sim 5$ Td. The colour code is BIAGI-v8.9 (——); BSR (——); HAYASHI (——); IST-LISBON (——); MORGAN (——); PHELPS (——); PUECH (——). The legend refers to the first author and year of publication of references reporting measurements shown in the figure.

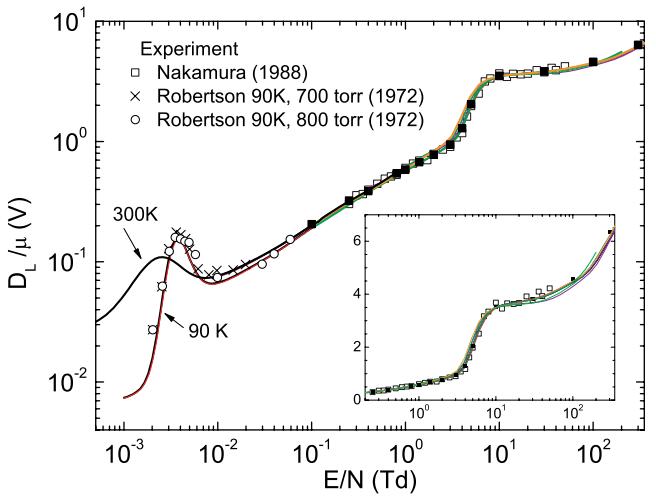

Figure 6. Comparisons of calculated and measured D_L/μ. The open symbols are measurements as indicated in the legend, the closed symbols (■) are Monte Carlo (MAGBOLTZ) results at 293 K and the lines are results of calculations using BOLSIG+. The ordinate in the inset is linear. The colour code is BIAGI-v8.9 (——); BSR (——); HAYASHI (——); IST-LISBON (——); MORGAN (——); PHELPS (——); PUECH (——). The measurements are referenced in the text.

the relation $v_d = \mu N \times E/N$, where E/N is the reduced electric field strength, μ is the electron mobility and N is the neutral density. The error in the reported values of E/N is quite small and so the conversion to mobility does not degrade the precision of the data.

Calculated and measured values of the reduced electron mobility versus E/N are shown in figure 5. The quoted error bars in the measurements of Robertson (1977) are less than 3% over the whole range. The very low E/N measurements of Pack and Phelps (1961) at 77 and 300 K have an estimated uncertainty of about 25% because of possible molecular impurities in the gas mixture (Robertson 1977), and, although they do not meet the criteria proposed in appendix I to be included in the comparisons with calculations, we include them here anyway because they illustrate the low-field dependence of the reduced mobility on gas temperature. The most recent experimental results shown in the figure are from Nakamura and Kurachi (1988) who reported a series of drift velocity measurements with an estimated error of 2% that cover a wide range of E/N.

The gas temperature has an influence only at very low E/N where the energy gained by the electrons in elastic collisions with the target atoms is important in the energy balance. Results below 0.1 Td are shown only for the BIAGI-v8.9 dataset; all others yield the same within the experimental error bars. The knee in the curve around 5 Td corresponds to the point where energy loss in inelastic collisions (see section 3.4) starts increasing very rapidly with E/N. The differences (<15%) among the calculations in the 5 to 20 Td region reflect the differences in the elastic momentum-transfer cross section near 10 eV and in the near-threshold behaviour of cross sections for the 1s levels. While these differences might seem small, they are sufficient to give a slight preference to the BIAGI-v8.9 and BSR datasets if we take the measurements of Nakamura and Kurachi (1988) as the reference conditions. Puech and Torchin (1986) used the drift velocity data of Kucukarpaci and Lucas (1981) as reference conditions in the development of the dataset in the PUECH database. These data are higher than the Nakamura and Kurachi data and their scatter is large in the region of the knee, as seen in the inset in the figure. The earlier datasets of PHELPS and MORGAN were most likely compiled using other data for electron mobility which may not have had the precision of the Nakamura and Kurachi data in the region of the knee. (See LXCat for other experimental data.)

We have confirmed that results from two-term Boltzmann and Monte Carlo calculations using MAGBOLTZ (Biagi 2011) agree to within a few per cent or better over the full range of E/N in the figure.

3.2. D_T/μ and D_L/μ

Other commonly measured swarm parameters include the ratios, D_T/μ and D_L/μ, where eD_T/μ is called the 'characteristic energy' and can be thought of as the potential energy through which an 'average' electron can diffuse against the electric field. Since the average electron energy is not easily accessible experimentally, eD_T/μ provides a very useful energy scale even though there is no simple relation between average energy and eD_T/μ except for the case of a Maxwellian eedf. It has long been recognized that D_T/μ and D_L/μ can be quite different and in argon at a few Td, the difference is a factor of 7 with D_T/μ being the larger (Wagner *et al* 1967).

Shown in figure 6 are comparisons of calculated and measured values of D_L/μ versus E/N over the range of values of E/N covering the measurements of Nakamura and Kurachi (1988), who assign an experimental error of 10% to their measurement and the low-field measurements of

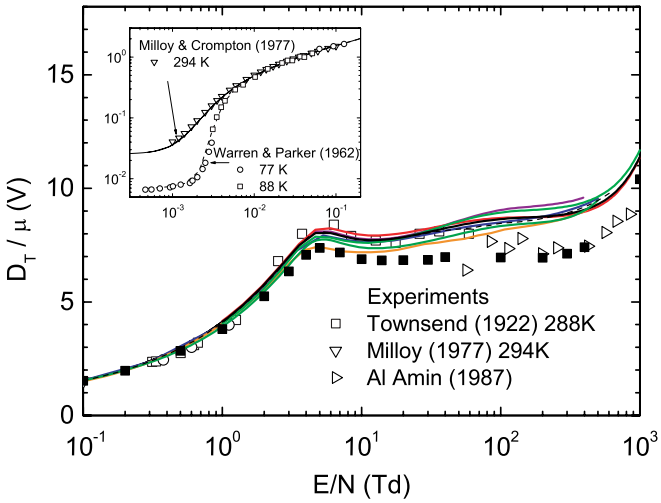

Figure 7. Measured and calculated values of D_T/μ versus E/N. The open symbols are measurements, the closed symbols (■) are Monte Carlo calculations and the lines are results from two-term Boltzmann calculations. The inset shows results at low E/N for 77, 88 and 288 K. The colour code is BIAGI-v8.9 (——); BIAGI-v7.1 (- - - -); BSR (——); HAYASHI (——); IST-LISBON (——); MORGAN (——); PHELPS (——); PUECH (——). The measurements are referenced in the text.

Robertson and Rees (1972) at 90 K. Actually, Nakamura and Kurachi report separately values of $D_L N$ and drift velocity; we have converted to D_L/μ for these comparisons. There is good agreement for all calculations with the measurements of Nakamura and Kurachi. Two sets of calculations are shown at 90 K (HAYASHI and BIAGI-v8.9) and these are in agreement with the experiments of Robertson and Rees, especially considering the comment in their paper that their values should be regarded as upper limits to the true values. The two-term Boltzmann calculations are in excellent agreement with the Monte Carlo results, which are shown in the full symbols in the figure. The gas temperature-dependent structure in D_L/μ at low field is caused by the Ramsauer minimum. That is, an electron swarm with an average energy on the low side of the Ramsauer minimum where the elastic momentum transfer is rapidly falling will see a large range of scattering lengths (and thus large longitudinal diffusion coefficient). When the electrons are mainly in the region of the minimum, they will have a smaller spread in scattering lengths. The change in slope around 3 Td is caused by the rapidly increasing influence of inelastic collisions past this point. At 300 K, the eedf is wider and the structure is less pronounced.

We show in figure 7 comparisons of calculated and measured values of D_T/μ versus E/N. Although the criteria outlined in appendix I for inclusion of experimental data in these comparisons are respected only for the Milloy and Crompton (1977a), the experimental results of Al-Amin and Lucas (1987) and the old measurements of Townsend and Bailey (1922, 1923) are shown in order to cover a wider range of E/N and gas temperature. Data from Warren and Parker (1962) at 77 K are shown in the inset.

Results from two-term Boltzmann calculations differ among the various datasets by some 10% for $E/N > 5$ Td but appear to be in overall satisfactory agreement with the measurements of Townsend and Bailey up to about 50 Td. The inadequacy of the two-term approximation for calculations of D_T/μ in gases with a Ramsauer minimum has previously been noted (see, for example, Hayashi (1987)). The existence of a deep Ramsauer minimum, even in an energy range far below thresholds for inelastic processes, introduces significant error in the two-term calculation of D_T/μ over a wide range of E/N. Results from a Monte Carlo simulation using the BIAGI-v8.9 dataset are also shown in figure 7. Indeed, these are some 25% lower than the two-term results for $E/N > 5$ Td calculated using the same cross section set and lower than the experimental results of Townsend and Bailey. Note that above 50 Td, the Monte Carlo calculations using the cross section set of BIAGI-v8.9 appear to be in agreement with the experimental results of Al-Amin and Lucas (1987) in spite of the considerable scatter in these measurements.

Certain datasets (PHELPS, MORGAN, IST-LISBON) have been compiled by adjusting the cross sections to give a good fit to calculated swarm parameters including the D_T/μ calculated using the two-term approximation. These cross section sets should subsequently be used in two-term calculations, and not in a Monte Carlo or multi-term calculation, and vice versa, if precision in the calculation of D_T/μ is required. In appendix A, Biagi points out that he was unable to fit both D_T/μ and D_L/μ in argon below 100 Td using his Monte Carlo code, and he chose to fit the more modern D_L/μ data rather than the early measurements of D_T/μ in compiling his BIAGI-v8.9 dataset for argon.

Calculated values of D_T/μ versus E/N are shown in the inset in figure 7 for 77, 88 and 294 K for low E/N, along with results from BOLSIG+ for the BIAGI-v8.9 dataset only—the other datasets lead to the same results. In the limit of zero electric field, the eedf should relax to a Maxwellian at the gas temperature and the characteristic energy should obey the Einstein relation, $D_T/\mu = k_B T_g/e$ where e is the electronic charge, k_B is the Boltzmann constant and T_g is the gas temperature. We see in the inset in figure 7 that this relation is indeed respected both in the experiments and in the calculations for very low E/N. However, this testifies more to the precision of the Boltzmann calculation than to the accuracy of the cross sections.

3.3. Reduced ionization coefficients

The reduced ionization (Townsend) coefficient, α_i/N, defined as the number of ionization events per unit distance in the drift direction normalized to the neutral number density, is a function of E/N. This quantity can be extracted from measurements of the anode current for different gap spacings in a parallel plane geometry and is very important in fluid modelling of low temperature plasmas because it describes the ionization balance.

Figure 8 compares measurements and two-term Boltzmann calculations (using the SST formulation, as mentioned above) of the reduced ionization coefficients using the different cross section datasets. A few results from Monte Carlo calculations are also shown by the closed symbols in figure 8 in order to confirm that the two-term results are reliable for

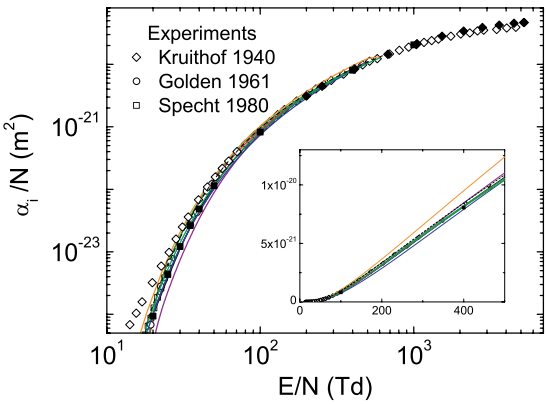

Figure 8. Measured and calculated reduced ionization coefficients. The solid lines are results from two-term Boltzmann calculations and the solid symbols (■) are from the Monte Carlo calculations using MAGBOLTZ (Biagi 2011). The colour code is BIAGI-v8.9 (——); BSR (——); HAYASHI (——); IST-LISBON (——); MORGAN (——); PHELPS (——); PUECH (——). The measurements are referenced in the text.

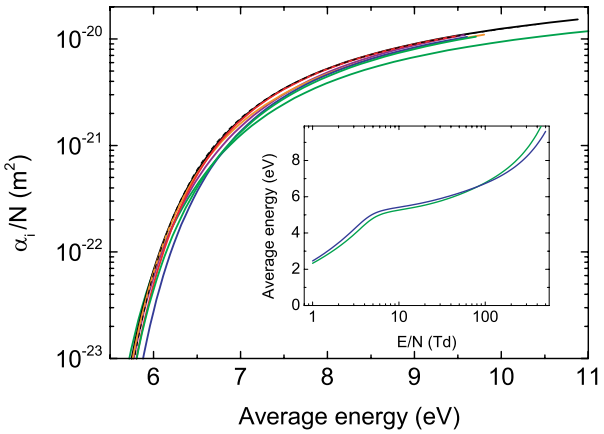

Figure 9. Reduced ionization coefficient versus average electron energy, calculated using a two-term Boltzmann solver. The inset shows the average energy versus E/N, and the colour code is BIAGI-v8.9 (——); BIAGI-v7.1 (- - - -); BSR (——); HAYASHI (——); IST-LISBON (——); MORGAN (——); PHELPS (——); PUECH (——).

the calculation of α_i/N. Of the experimental data available in the literature, we retained for these comparisons the measurements from Kruithof (1940), Golden and Fisher (1961) and Specht *et al* (1980). The Kruithof data differ from the others only at low E/N and this is most likely due to an additional Penning component in the older data. The inset is on a linear scale and serves to illustrate the small differences in the calculations. The eight, independently derived, and sometimes very different sets of cross sections yield values of the ionization coefficient within a few per cent of each other at 500 Td (except for the PUECH dataset which is about 20% higher than the others at this value of E/N). Because α_i/N is an average over the eedf, it depends on the combined influence of all collision events, as do all swarm data. This general agreement among the calculations using sometimes very different cross section sets serves to emphasize again the fact that fitting of cross sections sets to swarm data does not lead to a unique set of cross sections (Petrović *et al* 2007).

Although the ionization coefficients as functions of E/N in figure 8 seem to be in good agreement among themselves, differences are apparent when plotted as functions of average electron energy as shown in figure 9. The dependence of the swarm parameters on average electron energy cannot be compared directly to experiment because average electron energy is not a measurable quantity. Nevertheless, this is of interest because some fluid models of low-temperature plasmas include an equation for the average electron energy and parameterize the transport and Townsend coefficients as functions of average electron energy (Boeuf and Pitchford 1995) with a functional dependence the same as in swarm (uniform, constant field) conditions. The inset in figure 9 shows the calculated average electron energy versus E/N for the IST-LISBON and the BSR datasets which represent the limiting cases and except in the immediate vicinity of the cross over at about 80 Td, the other cases fall in between these two. Both α_i/N and average energy are averages over the eedf but with different weightings and hence they reflect different parts of the eedf. Comparisons of α_i/N versus average electron energy highlight differences between the results that are not so obvious in plots versus E/N. This point was first made many years ago by Frost and Phelps (1962) who determined sets of cross sections by using characteristic energy, eD_T/μ, rather than E/N as a parameter for comparisons of calculations and experiments.

A point to note is that BOLSIG+ cannot find a steady-state solution for E/N greater than some 500 to 700 Td, but depending on the dataset, when using the spatial growth model (SST). Monte Carlo simulations using the spatial growth model do not indicate any particularly unusual behaviour near the value of E/N where BOLSIG+ fails to converge. Using the temporal growth model (PT) BOLSIG+ finds solutions up to 1000 Td in helium and higher in the heavier noble gases. We have not fully understood the reason why the SST formulation in BOLSIG+ has no solution at high E/N, but it appears not to be a numerical issue. We suspect that it is caused by some fundamental incompatibility at high fields between the two-term approximation and the way the electron flux is renormalized in the SST formulation. As discussed in appendix J, the changing electron number density due to ionization (and attachment in electronegative gases) is accounted for in SST by renormalizing the electron flux whereas in PT the electron number density is renormalized. The same behaviour occurs in helium and neon (see Paper II) at lower values of E/N and in Kr and Xe at higher values of E/N (Paper III).

3.4. Excitation coefficients

Excitation coefficients for the metastable ($1s_5$ and $1s_3$) and resonance ($1s_4$ and $1s_2$) levels of argon by collisions with low-energy electrons were measured by Tachibana (1986) using a drift tube technique. An analysis of the measured time dependence of the absolute population densities of the excited levels yielded the excitation coefficients. These measurements provide further points for checking the cross section datasets. The four 'detailed' datasets and the

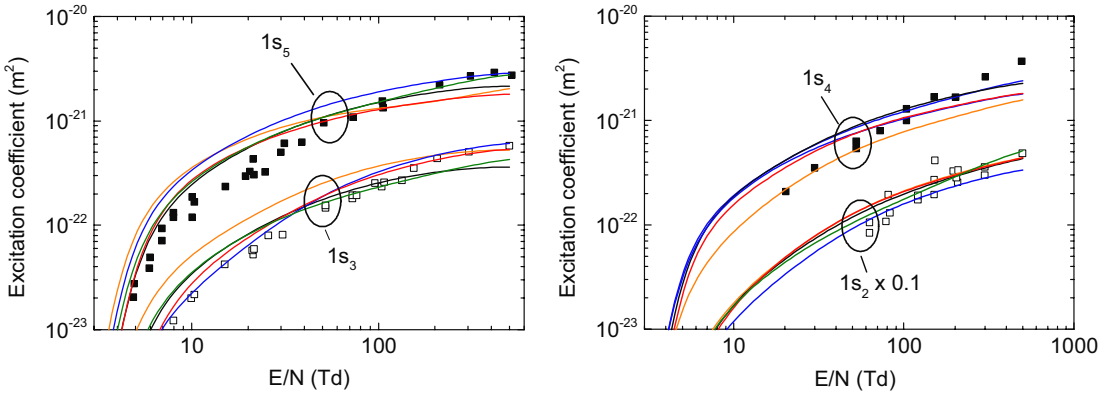

Figure 10. Measured (■, □) and calculated (lines) reduced excitation coefficients for 1s metastable (left) and resonance (right) levels. The colour code is BIAGI-v8.9 (——); BSR (——); HAYASHI (——); IST-LISBON (——); PUECH (——). The measurements are from Tachibana (1986).

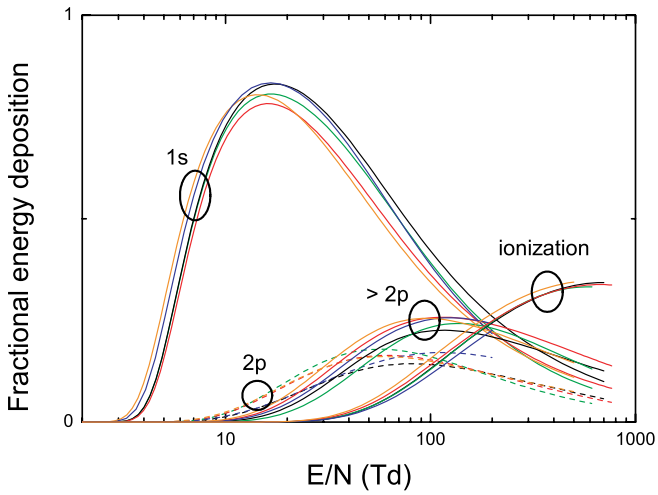

Figure 11. Fractional energy loss in excitation and ionization versus E/N calculated using cross sections from different databases. The colour code is BIAGI-v8.9 (——); BSR (——); HAYASHI (——); IST-LISBON (——); PUECH (——).

theoretical dataset of BSR were used to calculate the excitation coefficients for the comparisons with the measurements shown in figure 10. As emphasized by Tachibana, the excited states are populated by direct excitation and by cascading, and the cascading contribution must be taken into account in the comparisons. Tachibana's experiments were carried out at 300 Pa in an attempt to minimize contributions due to collisional cascading and the estimated error is the measured excitation coefficients ±25 to 30%. In our calculations, we consider radiative cascading only from the 2p levels, and the results shown in figure 10 were calculated using radiative transition probabilities from NIST (Wiese *et al* 1969). Previous comparisons of these measured excitations rates with calculations including cascading have been reported by Puech and Torchin (1986) and Yanguas-Gil *et al* (2005). These authors also considered cascading from excited states higher than the 2p levels and so are slightly different at high E/N from the results shown here.

The power deposited in the electrons by the electric field is equal to $\mu N \times (E/N)^2$. In the figure 11, we show the fraction of this power, as a function of E/N, that goes into excitation of different groups of levels—in excitation of the metastable and resonance (1s) levels, in excitation of the ten 2p levels, in excitation of all the higher levels, and in ionization. These results were calculated using BOLSIG+ using the four detailed, swarm-derived datasets and the theoretical BSR database.

At low E/N and up to about 100 Td, most of the electronic energy goes into excitation of the 1s levels. The fractional energy deposited in excitation of the 2p and higher levels is significant but never dominant. For E/N greater than about 200 Td, energy loss in ionization is the dominant component in the energy balance. Cascading contributions to the excitation coefficients of the 1s levels (figure 11) can only be important for $E/N > 100$ Td or so where a significant part of the electronic energy goes into the 2p and higher levels. The details of the fractional energy deposited in the different channels are dependent on the database chosen for the calculation, although the trends are the same in all results.

4. Recommendations and conclusions

The purposes of this paper have been to document the datasets available for electron scattering in argon that are presently available on the open-access website LXCat and to comment on their use in plasma modelling. We have compared the nine, independently determined datasets presently available on LXCat among themselves, and we have used eight of these in Boltzmann calculations to obtain swarm parameters for comparisons with measurements. The Boltzmann calculations were performed using BOLSIG+, a homogeneous two-term Boltzmann equation solver (Hagelaar and Pitchford 2005), as well as a Monte Carlo simulation (Biagi 2011) which is, in principle, equivalent to solving the Boltzmann equation for electrons without recourse to the two-term approximation (Longo 2000).

In spite of some significant differences in the details of the individual cross sections, most of these datasets yield swarm parameters is good agreement with the experiments chosen for the comparisons for the reasons given in appendix I. It is not surprising that the swarm-derived cross sections agree fairly well with experiment, but it is remarkable that the purely theoretical cross sections of Zatsarinny and Bartschat in the

BSR dataset yield swarm parameters in very good agreement experiments over the whole range considered here. The BSR data yield swarm parameters in good agreement with measurements in neon, too, (Paper II). The good agreement in argon is in spite of the fact that some of the theoretical cross sections are in disagreement (deviations of 30% or so) with beam measurements for certain processes. This illustrates that good comparisons with swarm parameters, while a minimum condition for use of a dataset in plasma modelling, are not sufficient to identify a unique cross section dataset. In addition to the comparisons with swarm parameters shown here in pure argon, further checks of the consistency of the cross section sets could include comparisons with swarm parameters in gas mixtures, comparisons of measured and calculated W values (energy loss per ion pair), confirmation that theoretical sum rules are respected, and more. Additional swarm experiments are desirable (particularly D_T/μ in argon), and, as mentioned by Petrović *et al* (2009) it could also be very useful to compare with experimental results in conditions where there is not a local equilibrium between electron energy gain and loss processes.

It has been shown that the results from BOLSIG+ (two-term Boltzmann solver) are in excellent agreement with Monte Carlo simulations for all values of E/N except for the calculation of the characteristic energy, eD_T/μ, for $E/N > 5$ Td where the two-term results are about 30% higher than results from the more accurate Monte Carlo simulations. It should be emphasized that in order to compare standard two-term Boltzmann solutions and Monte Carlo results, the important quantity to keep constant is $Q_{m,el}$. Wrong conclusions have been drawn in the literature regarding the accuracy of the two-term approximation because of failure to respect this point.

The cross sections datasets (those that are complete) for argon on LXCat can all be used to calculate steady-state eedfs for uniform fields and uniform background number density. These comparisons are the minimum tests that should be made before using cross section data for plasma modelling. The choice of which database to use then depends mainly on the question being asked—the 'simple' datasets are perfectly well adapted to calculations of eedfs and swarm parameters but are clearly inadequate in cases where detailed information about specific energy loss processes is being sought (e.g. excitation of metastable levels).

It is standard practice at the moment to neglect the higher order anisotropies in the scattering cross sections, partly because these have been shown to play a minor role in some cases but mainly because the full information is simply not often available. Note that standard two-term Boltzmann solvers can only take into account the isotropic and $\cos\theta$ components of elastic differential cross sections and only the isotropic part of the inelastic cross sections. Thus inclusion of higher order anisotropies in the calculations requires multi-term or Monte Carlo solution techniques. While neglect of anisotropic scattering is often adequate for calculations of swarm parameters for electrons, it is rarely so simple for ions. In both cases, more attention should be devoted to this issue. The need for more detail in the cross sections should be examined in particular for low pressure, non-equilibrium conditions where particle-in-cell/Monte Carlo is commonly used. We can make no statement about how well the cross section datasets in LXCat describe this situation.

Finally, we would like to recall that this work was carried out in the context of the GEC Plasma Data Exchange Project and that this project is open to all interested participants. And, new contributors to the LXCat site are always welcome. It is only through an active effort on the part of the members of the low-temperature plasma community that the accessibility of high-quality data for plasma modelling can be assured.

Acknowledgments

We thank Sanchita Chowdhury for her excellent technical assistance on many aspects of this work. The work of KB and OZ was supported by the United States National Science Foundation under grants No PHY-1068140 and No PHY-1212450, and by the XSEDE supercomputer allocation No TG-PHY-090031. The work of LLA and CMF was partially supported by Fundação para a Ciência e a Tecnologia, under Project Pest OE/SADG/LA0010/2011.

Appendix A. Comments on BIAGI-v7.1 and BIAGI-v8.9 databases (by Biagi)

The cross section sets for argon in both of these databases were derived from fitting to accurate drift velocity and diffusion measurements using double shutter drift tubes with variable drift distances (Nakamura and Kurachi 1988). This measurement technique, which is a differential technique in drift distance, tends to remove systematic errors in the measurements caused by end effects and non-equilibrium of the electron swarm. The cross sections in both datasets are identical up to 1.0 eV and are given analytically using a phase shift analysis from Petrović *et al* (1995). Details of this technique can also be found in Haddad and O'Malley (1982) and the fit is accurate to better than 0.3% to the experimental drift velocity measurements of Robertson (1977) at low E/N.

At higher values of E/N, the drift velocity measured by Nakamura and Kurachi (1988) is taken as the most accurate and both cross section sets fit well to these measurements with less than 1% deviations on average. The drift velocity at the highest E/N values of Nakamura and Kurachi depends not only on the elastic momentum-transfer cross section but also on the excitation cross sections of the lowest s-states. In the original derivation of the set 7.1 we used compatible values of the s-state cross sections to those used by Nakamura and Kurachi and as a result we obtained and used a similar elastic momentum-transfer cross section above 1.0 eV.

It became apparent after the publications of Allan *et al* (2006) that the cross sections for the s-states close to threshold were much higher than were used in the version 7.1 dataset. This fact and the need to model more accurately the light emission from excimers (Oliveira *et al* 2011) and the Penning transfers in argon gas mixtures (Sahin *et al* 2010) led to the

development of the cross section set 8.9 with a more accurate description of the level structure. The momentum-transfer cross section at the peak in version 8.9 is slightly higher than in 7.1 in order to compensate for the different excitation cross section.

The inelastic cross sections in the version 8.9 dataset were derived using the following constraints:

- The dipole allowed states were described by BEF scaling (Kim 2001, Kim 2007) with oscillator strengths from theory and experiment which had been published up to 2010. The agreement with theory and experiment is very good (Zatsarinny and Bartschat 2004, Allan *et al* 2006, and Berkowitz (2002). The total oscillator strength for all the used levels was only a few % below the total oscillator strength given by the TRK sum rule (Kuhn 1925, Reiche and Thomas 1925, Thomas 1925). The missing oscillator strength was then added into the dataset by adding an effective level with remaining oscillator strength.
- The analytical cross section fit to the BEF formula was only used above the resonance region. In the resonance region we used the cross section of Allan *et al* (2006) and scaled it to give a good fit to the light emission measurements of Tachibana (1986) and the reduced ionization coefficients measured by Kruithof (1940) for version 7.1 and by Kruithof (1940) and Specht *et al* (1980) for version 8.9.
- The triplet states that do not decay to the ground state have similar shape functional forms used to describe the cross sections, and their amplitudes were allowed to vary within the available experimental limits given mainly by electron scattering measurements from Jet Propulsion Laboratory (Leclair *et al* 1996).

The ionization cross section used was an average of the data from Rapp and Englander-Golden (1965) and the more recent data of Straub *et al* (1995). These measurements agree within their experimental errors of 3 to 6% which gives confidence that the ionization cross section would not be the limiting factor in the accuracy of the derived dataset.

The analysis showed that in the case of 7.1, with the smaller s-state excitation cross sections, the data of Kruithof could be fit over the full range of E/N with only a small deviation at the lowest values of E/N. This deviation could be ascribed to either errors in the 7.1 dataset or to errors in the measurements of Kruithof.

The larger s-state cross sections used in the 8.9 analysis made the deviation between experiment and calculation of the ionization rate at low E/N more severe and pointed to a likely explanation being the effect of impurities giving an additional Penning contribution in the Kruithof experiment. With this in mind we have now included the Specht *et al* measurements which included an analysis of Penning transfers at low field. The 8.9 analysis fits well to the Specht experimental data, merges into the Kruithof measurements at higher E/N, and is within an average of $\pm 3\%$ over the full E/N range.

The fitting process was also constrained by the light emission from the s and p levels of (Tachibana 1986). The values of the s-state cross section in the resonance region given by Allan *et al* (2006) were scaled by 0.85 to maintain experimental agreement within error bars both for the light emission and the ionization rate. The light emission measurements tended to push the scaling factor to smaller values and the ionization rate tended to push the scaling factor to higher values.

The 7.1 and 8.9 datasets were not adjusted to fit the experimental diffusion data but both accurately follow within experimental errors the low-field transverse diffusion measurements of Milloy and Crompton (1977a) and the higher electric field longitudinal diffusion measurements of Nakamura and Kurachi (1988).

The high field transverse diffusion measurements of Townsend and Bailey (1922) remain the only data that is not predicted well by these datasets. The plots in figure 7 showing agreement of the two-term calculations with these D_T/μ data are caused by a chance coincidence of the error introduced by the two-term approximation giving a contribution which fits the Townsend experiment. However, accurate multi-term and Monte Carlo calculations show that the Townsend diffusion data are not well fitted by any cross section set.

An option to include angular anisotropy in the cross sections based on a screened Coulomb potential model (Belenguer and Pitchford 1999, Okhrimovskyy *et al* 2002) has been included in the subroutine for argon in MAGBOLTZ versions posterior to 2006. The angular anisotropy, when included in the 8.9 data base, only has an observable effect only above 1000 Td. For fields below 1000 Td the angular effects, when treated consistently, change the drift velocity and diffusion by less than 1%.

Appendix B. Comments on the BSR database (by Bartschat)

The BSR results are an extension of the work originally described by Zatsarinny and Bartschat (2004). The extension is similar to that for e–Ne collisions published by Zatsarinny and Bartschat (2012a, 2012b). Briefly, the e–Ar collision system was modelled through a close-coupling expansion that included the lowest 31 physical target states of neutral argon, i.e. the $(3p^6)^1S_0$ ground state and the excited states with dominant configurations $3p^5 4s$ (four states), $3p^5 4p$ (ten states), $3p^5 3d$ (twelve states) and $3p^5 5s$ (five states), respectively. Compared to the original 31-state calculation (Zatsarinny and Bartschat 2004), another 469 pseudo-states were then added to the close-coupling expansion. These short-range states with a discrete energy spectrum serve as a numerical discretization of the target continuum and a coarse sampling of the high-lying infinite number of Rydberg states. Of the 500 states, 78 had energies below the first ionization threshold while the remaining 422 states lay above it. Relativistic effects were accounted for at the level of the semi-relativistic Breit–Pauli approximation, which should be sufficiently accurate for a relatively light target such as argon and the cross sections of interest for plasma applications. The close-coupling equations were solved by employing the B-spline R-matrix (BSR) method and the accompanying suite of computer codes

described by Zatsarinny (2006). For more information about theoretical methods for electron–atom collisions, we refer to the Paper IV written by Bartschat (2013) as part of this series.

These quantum mechanical calculations are fully *ab initio* and predict excitation energies slightly higher than those measured. The differences between theoretical and measured excitation energies are small (at the 0.1 eV level for the lower s and p excited states and at the 0.2 eV level or less for the higher excited states). For practical applications such as those discussed in the present paper, these differences have essentially no effect on the results.

Based on detailed comparisons between experimental data for state-resolved, highly differential (in energy and angle) observables, as well as the experience gained on this type of calculations over many years, we can make some general statements about the likely accuracy of these predictions. Specifically

- We believe the elastic and momentum-transfer cross sections to be accurate at the level of a few per cent. This assessment is supported by the excellent agreement seen in this paper between modelling predictions using these cross sections and the corresponding experimental data.
- The excitation results, especially for incident projectile energies above the ionization threshold and for weak, optically forbidden transitions, are very sensitive to details of the theoretical model. Models that only include discrete states, such as the 31-state calculation (Zatsarinny and Bartschat 2004), are expected to generally overestimate the true excitation cross sections. Our experience suggests that close-coupling, as a unitary theory that conserves the total flux, will try to simulate processes such as ionization by (incorrectly) redistributing the corresponding flux into the excitation channels. See also (Bartschat 2013). Similarly to what we found in two recent publications (Zatsarinny and Bartschat 2012a, 2012b) on e–Ne collisions, the predicted excitation cross sections were indeed significantly smaller in the 500-state (BSR-500) model than those obtained in the earlier 31-state (BSR-31) calculation. As discussed in section 2 of this paper, the BSR-500 cross sections are even somewhat lower than many experimental data, while the BSR-31 cross sections were certainly too large. We performed a number of checks to test the sensitivity of the results. These calculations, however, are computationally very demanding and expensive. They can only be carried out on massively parallel supercomputers, which puts a practical limit on the extent to which the convergence with the number of states in the close-coupling expansion, as well as other numerical parameters such as the R-matrix radius and the energy distribution of the pseudo-states, can be tested. Nevertheless, based on these tests, we expect the relatively large cross sections, especially those for optically allowed transitions, to be accurate within 20% for most energies. We note that direct experimental data, usually obtained from crossed-beam experiments, also carry large uncertainties with respect to the absolutely normalization.
- Total ionization cross sections can be estimated from the BSR-500 model by adding up all the excitation cross sections for the pseudo-states that lie above the ionization threshold. For details, see (Zatsarinny and Bartschat 2012a, 2012b, Bartschat 2013). As also discussed in section 2 above, our predictions for the total ionization cross section are lower than experiment by up to about 30% between threshold and the maximum of the cross section around 80 eV. Our tests so far suggest that the results are stable to better than 30%, and hence we can currently not explain the remaining discrepancies between the BSR results and the direct measurements of the ionization cross sections. However, assuming that at least the energy dependence of the experimental data is very reliable (more than the absolute normalization), it is likely that the BSR model needs to be further improved in this intermediate energy regime. Even more pseudo-states may be required in the energy region from threshold to a few times that energy. Unfortunately, we cannot perform such calculations at the present time, simply because of the limited available computational resources. Nevertheless, as demonstrated in this paper, using the set of BSR-500 cross sections for all elastic and inelastic processes reveals very good agreement with several of the measured plasma parameters.

Appendix C. Comments on the Hayashi database (by Pitchford and Phelps)

The late Professor Makoto Hayashi compiled bibliographies and recommended datasets for a number of gases and reported some these in a series of reports from the National Institute for Fusion Science in Japan and others in a book chapter (Hayashi 1987). These summarize results from his compilations of data undertaken while he was at Nagoya Institute of Technology and, after his retirement, at Gaseous Electronics Institute in Nagoya. The NIFS reports are available on-line at www.nifs.ac.jp/report/nifsdata.html. A separate database on LXCat was set up so as to include this trove of data from Hayashi in the Plasma Data Exchange Project. Some of the data attributed to Hayashi on LXCat were available in tabular form, but others were digitized by Morgan or Chowdhury from published curves. The argon data discussed in the present article are available in tabular form at the end of the Hayashi's 2003 NIFS report on argon (Hayashi 2003). His recommended cross sections in argon are dated 1991 and are accompanied by the comment 'I would like to improve these cross section values slightly'. In Hayashi (1987) he states that the cross sections were 'determined from available data from electron beam and electron swarm experiments via the Boltzmann equation and the Monte Carlo simulation method. The beam data were given highest priority, and theoretical values of cross sections were sometimes used'.

A somewhat modified set of Hayashi's argon cross sections, i.e. a higher momentum-transfer cross section at high energies, has been used in Monte Carlo calculations and yields electron transport and ionization coefficients that are approximately consistent with swarm experiments. See Kondo

and Nanbu (2000). For an earlier analysis see Nanbu and Kageyama (1996).

Appendix D. Comments on the IST-Lisbon database (by Alves)

The IST-Lisbon database contains the most up-to-date electron–neutral collisional data (together with the measured swarm parameters used to validate these data), resulting from the research effort of the Group of Gas Discharges and Gaseous Electronics with the IPFN/IST (Instituto de Plasmas e Fusão Nuclear/Instituto Superior Técnico), Lisbon, Portugal. The data correspond to complete sets of electron–neutral scattering cross sections from ground-state, and were validated against swarm parameters and reduced excitation/ionization coefficients by solving the two-term homogeneous electron Boltzmann equation.

The compilation and adjustment of our complete set of electron–neutral scattering cross sections from ground-state argon is reported in the following work: (Yanguas-Gil *et al* 2005). This paper presents detailed comparisons between our final set of cross sections and the ones proposed by other authors.

The elastic momentum-transfer cross section was obtained from Phelps ftp://jila.colorado.edu/collision-data/electronneutral/electron.txt (Yamabe *et al* 1983).

Direct excitation cross sections up to 100 eV were obtained from the following works:

- for the $4s_5$ and $4s_3$ metastable states, Khakoo *et al* (2004);
- for the $4s_4$ and $4s_2$ radiative states, Khakoo *et al* (2004). These cross sections were multiplied by a factor 0.5;
- for the 4p states (10 levels), Chilton *et al* (1998);
- for the 3 d, 3d′, 5s and 5s′ states (10 levels), Hayashi (2003);
- for the 5p states (10 levels), Weber *et al* (2003);
- for the 4 d, 6s and 4d′ states, only optically allowed transitions were considered using the expressions of Drawin in his 1967 report with the oscillator strengths given by Lee and Lu (1973).

The previous direct excitation cross sections were extended from 100 eV to 1 keV, by using analytical asymptotic expressions similar to those proposed by Bretagne *et al* (1986) and Bretagne *et al* (1982) (based on the time-dependent perturbation theory in conjunction with the first Born approximation).

For direct ionization we have adopted the cross section measured by Rapp and Englander-Golden (1965).

Cross sections were defined for energies up to 1000 eV using cubic-spline interpolation, and were adjusted (through the multiplication factor defined above) as to yield good agreement between calculated and measured swarm parameters (drift velocity, characteristic energy) and rates coefficients (the ionization coefficient, total excitation coefficients—including cascade contributions coherent with the proposed cross section set—for the 4s-metastable, the 4s-radiative and the 4p states), for E/N values below 500 Td.

Calculations used an in-house two-term homogeneous and stationary Boltzmann solver: (i) adopting 1000 points energy grids with constant step-sizes, varying between 0.002 and 1 eV according to the (low/high) E/N values considered; (ii) neglecting the production of secondary electrons (born in ionization events) in obtaining the eedf.

Appendix E. Comments on the Morgan database (by Pitchford)

These data were compiled over 30 years ago by WL Morgan and have been widely distributed through the community. They were available for many years on Morgan's Kinema Research Software website, and they were uploaded to the LXCat site in 2009.

The details of how Morgan's data in noble gases were compiled cannot be recalled at this point. However, the procedure was standard: a choice was made about the level of detail to be included for excitation (in this case, two excited levels to represent allowed and forbidden transitions), cross sections were estimated or guessed based on experiment and theory, and then these cross sections were adjusted by comparing measured swarm parameters with those calculated using ELENDIF, Morgan's two-term Boltzmann code (Morgan and Penetrante 1990). Morgan's aim was to have a set of cross sections adequate for modelling electron energy deposition in gases. Since these data have been used by many people over the years, we think it is useful to show comparisons with the more recently compiled or calculated datasets.

The maximum energy in the data table or the elastic momentum-transfer cross section in the Morgan database is 75 eV and it is lower in the heavier noble gases. The calculations reported here were done using the default extrapolation scheme in BOLSIG+ assuming that cross sections for energies higher than the last entry in the tables decrease like $\log(\varepsilon)/\varepsilon$ where ε is electron energy, consistent with the high-energy limit for cross sections for allowed transitions in the Born approximation.

Appendix F. Comments on the RDW method used to calculate the cross sections in the NGFSRDW database (by Stauffer)

The RDW method (Zuo *et al* 1991) is based on solutions of the Dirac equations, both for the bound state wave functions as well as the scattered wave. This provides several advantages over the usual Schrödinger (non-relativistic) approach. The bound target states are calculated by the multiconfiguration Dirac–Fock method which provides distinct wave functions and energy levels for each of the fine-structure levels. For example, there are separate orbitals for p-electrons with total (orbital plus spin) angular momentum $j = 1/2$ and 3/2. The distorted waves are solutions of the Dirac equations including the static potential of the target and treating exchange with the bound state by antisymmetrization of the total wave function. The spin of the electron appears explicitly so that all one-electron relativistic effects, such as spin–orbit coupling, are automatically included.

Our calculations yield different cross sections for each fine-structure transition. These have different high-energy behaviour depending on the total angular momenta of the initial and final states. In particular, for forbidden transitions the energy dependence is different if the transition can proceed by a direct collision or only by exchange with the incident electron.

Cross sections have been calculated for excitation of the $3p^6$ ground state to the various excited fine-structure levels of the $3p^5 4s$ configuration (Khakoo *et al* 2004), the $3p^5 4p$ configuration (Kaur *et al* 1998) as well as the $3p^5 3d$, $3p^5 5s$ and $3p^5 5p$ configurations (Gangwar *et al* 2010). Various cross sections for transitions from excited levels have also been calculated and are available in the LXCat database. Analytic formulas are provided in these references which allow the cross sections to be calculated at higher energies (generally greater than 50 eV).

All of these cross sections have been used in a collisional–radiative model to calculate the population densities of the various excited states of a low-temperature argon plasma (Gangwar *et al* 2012) using a Maxwellian distribution for the free electrons.

Distorted-wave methods are generally reliable for medium and high-energy electron excitations. We have found the RDW method produces reliable cross section in most cases for incident electron energies of three times the excitation energies and higher. Thus for excitation of the ground states of the noble gases we would expect our cross sections to be reasonably accurate for energies above 25 or 30 eV. Since the thresholds for transitions from excited states are much smaller, these cross sections are valid for smaller energies. Transitions that involve direct excitation are more accurate than those that can only be excited by exchange reactions. In order to have a consistent set of cross sections for the collisional–radiative models, we have calculated RDW cross sections down to threshold and results at these energies are included in the LXCat database for completeness.

Appendix G. Comments on the Phelps database (by Phelps)

The original version of the cross section set available at LXCat was based on Frost and Phelps (1964) as modified in Tachibana and Phelps (1981). It used the momentum-transfer cross section of Milloy *et al* (1977b) for electron energies below 4 eV, the momentum-transfer cross section of Fletcher and Burch (1972) at energies above 8 eV, the total excitation cross section of Schaper and Scheibner (1969), and the ionization cross section of Smith (1930). The effective momentum-transfer cross section is the momentum-transfer cross section that should be used in the two-term spherical harmonic expansion to account for the effect of inelastic collisions in the f1 equation (the first anisotropy in the Legendre expansion of the Boltzmann equation). It is equal to the sum of the elastic momentum-transfer cross section and the sum of the 'total' (angular integrated) inelastic cross sections. For discussions of this point, see Baraff and Buchsbaum (1963) and Pitchford and Phelps (1982). When extending the cross section to 10 keV, based on Schram *et al* (1965) the cross sections are about 10% lower than those of Eggarter (1975) and those based on Peterson and Allen (1972). It should be noted that this dataset uses linear interpolation in order to avoid negative cross sections sometimes obtained with polynomial interpolation at the widely spaced entries at high energies. The dataset is derived for use with the two-term spherical harmonic expansion technique for solving the electron Boltzmann equation.

The cross section set available at LXCat has been tested through the comparison of calculated transport and reaction rate coefficients with experiment in pure Ar for $1 <= E/N <= 3000$ Td. The calculated coefficients are listed in the file eletrans.txt at http://jila.colorado.edu/~avp/collision_data/electronneutral/ (also in the Notes section on LXCat). Only the very early comparison with experiment in Frost and Phelps (1964) got published. The file electron.txt contains a procedure for obtaining rate coefficients and spatial excitation coefficients for the excitation of the 2p9 (811.5 nm) level, the 2p7 level (810.4 nm) and the 2s and 3 d levels.

Because of its very limited set of excitation cross sections, this cross section set is primarily of use in modelling electron behaviour at low E/N in Ar and in mixtures being used to study low-energy processes, such as rotational and vibrational excitation with added molecular gases or of the electron transport, excitation, and ionization with added low-ionization-potential metal vapours.

Appendix H. Comments on the Puech database

The article by Puech and Torchin (1986) describes in detail the procedure used for the compilation and consistency checking of this cross section set by comparisons with selected experiments.

Appendix I. Guidelines for selection of experimental data used for comparisons in this series of papers (by Biagi)

The guidelines listed here have been applied (more or less rigorously) in the present paper and in the two companion papers on He/Ne and on Kr/Xe to determine which experimental data are chosen for comparisons with the calculations.

(1) The datasets chosen should span a wide range of values of E/N and be at closely spaced values of E/N. Statistical or systematic errors would then show up as deviations from smoothness in the data.
(2) Where available we limit our comparisons to those experiments which measure at multiple drift distances within the same apparatus thus removing end effects and non-equilibrium issues.
(3) The measurements at the Ion Diffusion Unit at Australian National University (see for example, Robertson 1977) showed that the sensitivity of the measurements drift velocity to impurities can be large. For drift velocities, I propose that the best choice is to exclude data before

the late 1960s as the measurements were done with up to 20 ppm of impurities in the gases. The drift velocity measurements are the best test of cross sections measurements since they are the most accurate. Thus, we limit the comparisons to measurements to those with ±1% statistical and systematic errors or better where possible.

(4) The transverse diffusion measurements from the Ion Diffusion Unit at Australian National University with systematic and statistical accuracies of ±3% are so far superior to any other measurements and should be taken as the standard (for argon, Milloy and Crompton, 1977a). The transverse diffusion is mainly important in the constraint it applies to the derived cross section at the Ramsauer minimum

(5) We retain the longitudinal diffusion, D_L, measured by Nakamura and collaborators (see, for example, Nakamura and Kurachi (1988)) in a differential manner as these are the only high precision data in the noble gases. Note that these data extend to higher fields than most transverse diffusion measurements. For comparisons, we have converted these data to D_L/μ, using values of the drift velocity measured in the same experiments.

(6) Many of the measurements of the ionization coefficients after 1970 were measured over a restricted electric field and do not extend as high as the Kruithof data from 1937 (Kruithof and Penning 1937) and 1940 (Kruithof 1940). The latter Kruithof data are taken as a standard with the knowledge that there may be a contribution at low electric fields from Penning ionization of impurities. The errors in the Kruithof data are taken from the publication as ±4%. At low electric field the data of Specht *et al* (1980) give an approximate estimate of the impurity sensitivity of the ionization coefficient.

Appendix J. A brief overview of solution techniques used for calculations of swarm parameters (by Pitchford)

Two methods are used here for the analysis—a two-term Boltzmann solver and a Monte Carlo simulation (which is supposed to be equivalent to solving the Boltzmann equation without the two-term assumption). The Monte Carlo calculations were performed using MAGBOLTZ (Biagi 2011) and spot checks were made using the independently developed Monte Carlo simulation of Hagelaar. The determination of the swarm parameters from the Monte Carlo simulations is standard (Boeuf and Marode 1982, Penetrante *et al* 1985, Dujko *et al* 2008) and will not be discussed further.

The Boltzmann calculations reported here are also standard, but will be briefly developed here. Calculations reported above used the freeware package BOLSIG+ (Hagelaar and Pitchford 2005), but the option to calculate $D_L N$ is only included in versions later than September 2011. BOLSIG+ is a 'two-term' code making a standard set of approximations. The main approximations are that the electron velocity distribution function (evdf) is determined by a local balance between energy gained from the field and energy lost in collisions so that the shape of the distribution function is independent of space and time. This is satisfied for swarm conditions where the electric field is uniform, the background gas density is uniform, and boundary effects have been removed (by, for example, making measurements for different electrode spacings). The further assumption of cylindrical symmetry allows us to reduce the dimensionality the evdf such that it depends only on the speed and the angle between the velocity vector and the direction of acceleration in the electric field. 'Two-term' means that the angular dependence of the velocity has been expanded in Legendre functions and that only the first two terms have been retained. This procedure leads to a velocity distribution function

$$f(\boldsymbol{v}) = f_0(v) + f_1(v)\cos\theta, \tag{J1}$$

where f_0 is the isotropic component (or energy distribution function) and θ is the angle between the electron velocity and its acceleration in the electric field.

BOLSIG+ can be downloaded from www.bolsig.laplace.univ-tlse. A simplified version can be run on-line from the LXCat site. The on-line version does not have the flexibility of the freeware version—it is intended simply to give visitors to the LXCat site a quick estimate of swarm parameters. All calculations reported here used the default settings in BOLSIG+ for the numerical details (number of points in energy and grid spacing), linear interpolation is used to find values of cross section from tabulated data, and cross sections are assumed to decrease like $\log(\varepsilon)/\varepsilon$ energies, ε, past the maximum tabulated values. Secondary electrons born in ionization events are assumed to share equally the excess energy over the ionization potential.

Input to the Boltzmann solver includes elastic momentum transfer and total excitation and ionization cross sections. The effective momentum-transfer cross section, $Q_{m,eff}$ appears naturally in the collision term in the Boltzmann equation when the angular dependence of the velocity is expanded in Legendre polynomials and when anisotropies in the inelastic cross sections are neglected. $Q_{m,eff}$ is then equal to $Q_{m,el} + \sum Q_k + Q_i$, where Q_i is the total ionization cross section and the sum is over all inelastic processes, k, each with a total (angle integrated) cross section Q_k. In order to compare Boltzmann and Monte Carlo results, the Monte Carlo simulation should use $Q_{m,el}$ for elastic scattering but with a scattering angle after collisions chosen from an isotropic distribution.

At high E/N when ionization becomes important, it is necessary to distinguish among the ways that the growing number of electrons can be accounted for in the Boltzmann equation. That is, in swarm conditions, the eedf has a constant shape, independent of space and time, but its magnitude depends electron number density growth or decay due to ionization or attachment. How the changing magnitude is accounted for in the analysis (e.g. exponential temporal growth, exponential spatial growth, or a combination of both) depends on the experimental configuration under study.

Two simple experimental configurations are SST and PT. SST is a common configuration used to measure α_i/N and D_T/μ and the distinguishing feature is the assumption of exponential growth (or decay) of electron flux with distance from the cathode. In the equivalent Boltzmann equation, the

space derivative of the electron velocity distribution function is replaced by $\alpha_i f_{SST}(\boldsymbol{v})$, the product of the spatial growth constant (Townsend ionization coefficient) and the velocity distribution function. Thus the Boltzmann equation relevant for analysis of SST measurements can be written as:

$$\alpha_i v_z f_{SST}(\boldsymbol{v}) + a_z \frac{\partial f_{SST}(\boldsymbol{v})}{\partial v_z} = C[f_{SST}(\boldsymbol{v})], \qquad \text{(J2)}$$

where C is the collision operator and the acceleration in the electric field $a = -e\boldsymbol{E}/m$ is supposed to be in the z direction. f_{SST} is the electron velocity distribution function in the SST configuration.

PT is a configuration commonly used to measure drift velocity, v_d, and $D_L N$. The measured quantity is the voltage drop across an external series resistor following the release of a pulse of electrons from the cathode. In this case, the relevant Boltzmann equation is derived by setting the space derivate to zero and replacing the time derivative by $\nu_i f_{PT}(\boldsymbol{v})$. In the PT configuration, the Boltzmann equation can be written as:

$$\nu_i f_{PT}(\boldsymbol{v}) + a_z \frac{\partial f_{PT}(\boldsymbol{v})}{\partial v_z} = C[f_{PT}(\boldsymbol{v})], \qquad \text{(J3)}$$

where ν_i is the ionization frequency averaged over the distribution function. The ionization rate coefficient k_i is equal to ν_i/N.

With these assumptions, the Boltzmann equation reduces to a convection–diffusion continuity-equation with a non-local source term in energy space, which is discretized by an exponential scheme and solved for f_{PT} or f_{SST} by a standard matrix inversion technique in BOLSIG+.

When the electron number density is constant, there is no difference between equations (J2) and (J3) and no dependence on the experimental configuration. However, when ionization or attachment is present, f_{PT} is different from f_{SST}. The differences are such that the average electron energy in the SST configuration is lower because the electron density gradient in the direction of the field leads to diffusion cooling when ionization is present (or heating in the case of attachment). The calculated $D_T N$ is essentially unaffected by the assumed configuration, with a maximum difference of about 2% at 500 Td in argon whereas the differences in the calculated values of μN and α/N increase with increasing E/N from zero below 50 Td to 10 and 12% for the μN and α/N respectively at 500 Td in argon. The PT results for α/N are sensibly higher than those for SST where the average energy is lower. While these quantities can all be calculated (except $D_L N$ for SST—see below), it is hard to imagine how to extract values of $D_T N$ from measurements in a PT configuration or μN or $D_L N$ in a SST configuration. PT and SST are two simple experimental configurations; there are others for which the space and time dependence must both be considered (Tagashira *et al* 1977).

Integrals over f_0 (eedf) yield μN and $D_T N$ (equations (55) and (56), respectively in Hagelaar and Pitchford (2005)) and α_i/N (equation (66) or (67) for SST and PT, respectively). $D_T N$ in the notation here is identical to DN in equation (56) of Hagelaar. $D_L N$ is calculated for the PT configuration by following the standard procedure (Kumar *et al* 1980) of expanding the full electron velocity distribution function, $f^*(\boldsymbol{r}, \boldsymbol{v}, t)$ in powers of the gradient of the electron density in order to separate the space and dependencies. A Boltzmann equation can then be derived for $g_z^*(\boldsymbol{v}, t)$, the longitudinal component of the vector multiplying the first power of the electron density gradient. Taking into account the assumed exponential growth (or decay) of the electron density with time with a growth constant ν_i, $g_z^*(\boldsymbol{v}, t)$ is expressed as $\nu_i g_z(\boldsymbol{v})$ and we use a two-term expansion to solve for $g_z(\boldsymbol{v})$. $D_L N$ is calculated as an integral over $g_z(\boldsymbol{v})$. See equation (8) in Pitchford and Phelps (1981) for the derivation of $g_z(\boldsymbol{v})$ and equation (5) in that reference for the definition of $D_L N$.

References

Al-Amin S A J and Lucas J 1987 *J. Phys. D: Appl. Phys.* **20** 1590

Allan M, Zatsarinny O and Bartschat K 2006 *Phys. Rev.* A **74** 030701

Alves L L, Bartschat K, Biagi S F, Bordage M C, Pitchford L C, Ferreira C M, Hagelaar G J M, Morgan W L, Pancheshnyi S, Phelps A V, Puech V and Zatsarinny O 2013 *J. Phys. D: Appl. Phys.* **46** 334002

Baraff G A and Buchsbaum S J 1963 *Phys. Rev.* **130** 1007

Bartschat K 2013 *J. Phys. D: Appl. Phys.* **46** 334004

Belenguer Ph and Pitchford L C 1999 *J. Appl. Phys.* **86** 4780

Berkowitz J 2002 *Atomic and Molecular Photoabsorption: Absolute Total Cross Sections* (London/San Diego, CA: Academic)

Biagi S F 2011 *MAGBOLTZ* version 8.97, a Monte Carlo code http://consult.cern.ch/writeup/magboltz

Boeuf J P and Marode E 1982 *J. Phys. D: Appl. Phys.* **15** 2169

Boeuf J P and Pitchford L C 1995 *Phys. Rev.* E **51** 1376

Bordage M C, Biagi S F, Alves L L, Bartschat K, Chowdhury S, Pitchford L C, Hagelaar G J M, Morgan W L, Puech V and Zatsarinny O 2013 *J. Phys. D: Appl. Phys.* **46** 334003

Bretagne J, Callède G, Legentil M and Puech V 1986 *J. Phys. D: Appl. Phys.* **19** 761

Bretagne J, Godart J and Puech V 1982 *J. Phys. D: Appl. Phys.* **15** 2205

Chilton J E, Boffard J B, Schappe R S and Lin C C 1998 *Phys. Rev.* A **57** 267

Chutjian A and Cartwright D C 1981 *Phys. Rev.* A **23** 2178

Drawin H W 1967 *Fontenay-aux-Roses Report* Report No EUR-CEA-FC-383, unpublished

Dujko S, White R D and Petrović Z 2008 *J. Phys. D: Appl. Phys.* **41** 245205

Dutton J 1975 *J. Phys. Chem. Ref. Data* **4** 577

Eggarter E 1975 *J. Chem. Phys.* **62** 833

Fletcher J and Burch D S 1972 *J. Phys. D: Appl. Phys.* **5** 2037

Frost L S and Phelps A V 1962 *Phys. Rev.* **127** 1621

Frost L S and Phelps A V 1964 *Phys. Rev.* **136** 1538

Gallagher J W, Beaty E C, Dutton J and Pitchford L C 1983 *J. Phys. Chem. Ref. Data* **12** 109

Gangwar R K, Sharma L, Srivastava R and Stauffer A D 2010 *Phys. Rev.* A **81** 052707

Gangwar R K, Sharma L, Srivastava R and Stauffer A D 2012 *J. Appl. Phys.* **111** 053307

Gargioni E and Grosswendt B 2008 *Rev. Mod. Phys.* **80** 451

Golden D E and Fisher L H 1961 *Phys. Rev.* **123** 1079

Haddad G N and O'Malley T F 1982 *Aust. J. Phys.* **35** 35

Hagelaar G J M and Pitchford L C 2005 *Plasma Sources Sci. Technol.* **14** 722. An executable version of the BOLSIG+ code can be downloaded from www.bolsig.laplace.univ-tlse.fr

Hayashi M 1987 Electron collsion cross sections for molecules determined from beam and swarm data *Swarm Studies and Inelastic Electron–Molecule Collisions* ed L C Pitchford *et al* (New York: Springer)

Hayashi M 2003 Bibliography of electron and photon cross sections with atoms and molecules published in the 20th century, report NIFS-DAT-72 of the National Institute for Fusion Science of Japan
Hernandez-Avila J L, Basurto E and de Urquijo J 2004 *J. Phys. D: Appl. Phys.* **37** 3088
Huxley L G H and Crompton R W 1974 *The Diffusion and Drift of Electrons in Gases* (New York: Wiley-interscience)
Kaur S, Srivastava R, McEachran R P and Stauffer A D 1998 *J. Phys. B: At. Mol. Opt. Phys.* **31** 4833
Khakoo M A *et al* 2004 *J. Phys. B: At. Mol. Opt. Phys.* **37** 247
Kim Y-K 2001 *Phys. Rev.* A **64** 032713
Kim Y-K 2007 *J. Chem. Phys.* **126** 064305
Kondo S and Nanbu K 2000 *Rep. Inst. Fluid Sci.* **12** 101
Kruithof A A 1940 *Physica* **7** 519
Kruithof A A and Penning F M 1937 *Physica* **4** 0430
Kucukarpaci H N and Lucas J 1981 *J. Phys. D: Appl. Phys.* **14** 2001
Kuhn W 1925 *Z. Phys.* **33** 408
Kumar K, Skullerud H R and Robson R E 1980 *Aust. J. Phys.* **33** 343
Leclair L R, Trajmar S, Khakoo M A and Nickel J C 1996 *Rev. Sci. Instrum.* **67** 1753
Lee C M and Lu K T 1973 *Phys. Rev.* A **8** 1241
Longo S 2000 *Plasma Sources Sci. Technol.* **9** 468
Luft P E 1975 *JILA Information Center Report* No 14, University of Colorado, unpublished
Milloy H B and Crompton R W 1977a *Aust. J. Phys.* **30** 51
Milloy H B, Crompton R W, Rees J A and Robertson A G 1977b *Aust. J. Phys.* **30** 61
Morgan W L and Penetrante B M 1990 *Comput. Phys. Commun.* **58** 127
Morgan W L, Winstead C and McKoy B V 2001 *J. Appl. Phys.* **90** 2009
Nakamura Y and Kurachi M 1988 *J. Phys. D: Appl. Phys.* **21** 718
Nanbu K and Kageyama J 1996 *Vacuum* **47** 1031
Okhrimovskyy A, Bogaerts A and Gijbels R 2002 *Phys. Rev.* E **65** 037402
Oliveira C A B, Schindler H, Veenhof R, Biagi S, Monteiro C M B, don Santos J M F, Ferreira A L and Veloso J F C A 2011 *Phys. Lett.* B **703** 217
Pack J L and Phelps A V 1961 *Phys. Rev.* **121** 798
Pancheshnyi S, Biagi S F, Bordage M C, Hagelaar G J L, Morgan W L, Phelps A V and Pitchford L C 2012 *Chem. Phys.* **398** 148
Penetrante B M, Bardsley J N and Pitchford L C 1985 *J. Phys. D: Appl. Phys.* **18** 1087
Peterson L R and Allen J E 1972 *J. Chem. Phys.* **56** 6068
Petrović Z L, Dujko S, Marić D, Malović G, Nikitović Ž, Šašić O, Jovanović J, Stojanović V and Radmilović-Rađenović M 2009 *J. Phys. D: Appl. Phys.* **42** 194002
Petrović Z L, O'Malley T F and Crompton R W 1995 *J. Phys. B: At. Mol. Opt. Phys.* **28** 3309
Petrović Z L, Šuvakov M, Nikitović Ž, Dujko S, Šašić O, Jovanović J, Malović G and Stojanović V 2007 *Plasma Sources Sci. Technol.* **16** S1
Phelps A V 1997 ftp://jila.colorado.edu/collision-data/electronneutral/electron.txt. All electron scattering cross section datasets on this site have been uploaded to the LXCat site
Phelps A V and Pitchford L C 1985 *Phys. Rev.* A **31** 2932
Pitchford L C and Phelps A V 1982 *Phys. Rev.* A **25** 540
Puech V and Torchin L 1986 *J. Phys. D: Appl. Phys.* **19** 2309
Rapp D and Englander-Golden P 1965 *J. Chem. Phys.* **43** 1464
Ralchenko Y, Janev R K, Kato T, Fursa D V, Bray I and De Heer F J 2008 *At. Data Nucl. Data Tables* **94** 603
Reiche F and Thomas W 1925 *Z. Phys.* **34** 510
Robertson A G 1977 *Aust. J. Phys.* **30** 39
Robertson A G and Rees J A 1972 *Aust. J. Phys.* **25** 637
Şahin Ö, Tapan İ, Özmutlu E N and Veenhof R 2010 *J. Inst.* **5** P05002
Samukawa S *et al* 2012 *J. Phys. D: Appl. Phys.* **45** 253001
Schaper M and Scheibner H 1969 *Beitr. Plasma Phys.* **9** 45
Schram B L, De Heer F J, Van der Wiel M J and Kistermacher J 1965 *Physica* **31** 94
Smith P T 1930 *Phys. Rev.* **36** 1293
Specht L T, Lawton S A and DeTemple T A 1980 *J. Appl. Phys.* **51** 166
Straub H C, Renault P, Lindsay B G, Smith K A and Stebbings R F 1995 *Phys. Rev.* A **52** 1115
Tachibana K 1986 *Phys. Rev.* A **34** 1007
Tachibana K and Phelps A V 1981 *J. Chem. Phys.* **75** 3315
Tagashira H, Sakai Y and Sakamoto S 1977 *J. Phys. D: Appl. Phys.* **10** 1051
Thomas W 1925 *Naturwissenchaften* **13** 627
Townsend J S and Bailey V A 1922 *Phil. Mag.* **43** 593
Townsend J S and Bailey V A 1923 *Phil. Mag.* **46** 657
Wagner E B, Davis F J and Hurst G S 1967 *J. Chem. Phys.* **47** 3138
Warren R W and Parker J H Jr 1962 *Phys. Rev.* **128** 2661
Weber T, Boffard J B and Lin C C 2003 *Phys. Rev.* A **68** 032719
Wetzel R C, Baiocchi F A, Hayes T R and Freund R S 1987 *Phys. Rev.* A **35** 559
White R D, Robson R E, Schmidt B and Morrison M A 2003 *J. Phys. D: Appl. Phys.* **36** 3125
Wiese W L, Smith M W and Miles B M 1969 A*tomic Transition Probabilities* vol 2 (Washington, DC: US Department of Commerce)
Yamabe C, Buckman S J and Phelps A V 1983 *Phys. Rev.* A **27** 1345
Yanguas-Gil Á, Cotrino J and Alves L L 2005 *J. Phys. D: Appl. Phys.* **38** 1588
Zatsarinny O 2006 *Comput. Phys. Commun.* **174** 273
Zatsarinny O and Bartschat K 2004 *J. Phys. B: At. Mol. Opt. Phys.* **37** 4693
Zatsarinny O and Bartschat K 2012a *Phys. Rev.* A **86** 022717
Zatsarinny O and Bartschat K 2012b *Phys. Rev.* A **85** 062710
Zuo T, McEachran R P and Stauffer A D 1991 *J. Phys. B: At. Mol. Opt. Phys.* **24** 2853